

CHAPTER 26

Some Characteristics of Breaking Waves by

Fredric Raichlen¹ and Panos Papanicolaou²

INTRODUCTION

In recent years there has been a surge in coastal engineering research devoted to various aspects of breaking waves including their kinematics at and after breaking. For a review of certain aspects of this field the interested reader is referred to Peregrine (1983) and Battjes (1988); in this discussion only certain publications pertinent to this investigation will be mentioned briefly.

With the advent of laser-Doppler velocimetry (LDV) a number of investigators have measured the internal velocities of waves both before, at, and after breaking. For example, Nadaoka (1986) measured the velocities in the shoaling region under periodic breaking shallow water waves. This extensive study of the nearshore regions resulted in vector diagrams which described very well several spatial aspects of the flow shoreward of breaking. Skjelbreia (1987) also used LDV techniques to define the kinematic characteristics of breaking solitary waves. Measurements were made of the water particle velocities under spilling and plunging breaking waves both very near breaking and after breaking, close to the water surface and to the bottom. A high degree of reproducibility was possible with the laboratory wave generation system used so experiments were conducted at different locations with essentially the same wave; this will be discussed more fully later. Skjelbreia (1987) also presented vector diagrams of the velocities under plunging and spilling solitary breakers. These measurements when compared to those of Nadaoka (1986) raise several questions regarding similarities and differences between breaking oscillatory waves and waves of translation. In addition to detailed kinematic measurements, a macroscopic view of shoaling solitary waves was also taken by Skjelbreia (1987) yielding results on the variation of the wave height with distance both before and after breaking. Although there has been a considerable amount of work along these lines in the past, observations of the changes in the wave at and after breaking are still quite useful in developing an overall understanding of the breaking process.

Other investigators have presented experimental and analytical studies dealing with waves in the regions at and just after breaking. For example, Horikawa and Kuo (1966) presented the results of experiments on the change in height of periodic waves after breaking. They, Dally et al (1984), and others used these data to compare to analytical approaches to this problem with some degree of success. Svendsen et al (1978) and Svendsen (1984) also gave attention to the decrease in wave height which was associated with wave breaking and the subsequent propagation of the broken wave. Svendsen et al (1978) have defined several different regions after breaking to describe the wave characteristics in the surf zone: an outer region where there is a rapid change in wave shape, an inner region where changes are slow and the front part of the wave resembles a periodic bore, and the region of runup of the wave on the beach. The concept of the

¹Professor of Civil Engr., W.M.Keck Lab of Hydr. and Water Res., California Institute of Tech., Pasadena, CA 91125 USA

²Post-Grad. Res. Engr. UC San Diego, Dept. of AMES/INLS, B-010, La Jolla, CA 92093, USA

changing wave shape as an important aspect of the decrease of wave height after breaking was discussed by Svendsen (1984). In this connection it was suggested by him that a smaller percentage of the decrease in wave height after breaking is due to energy dissipation associated with the roller formation at breaking (and the concomitant turbulence generated) compared to that due to the change in the shape of the wave, i.e., the general collapse of the wave with distance after breaking. Svendsen (1984) applied estimates of the roller size measured by Duncan (1981), who formed a breaker behind a towed hydrofoil, to the question of the energy dissipation in a breaking wave; this will be discussed more fully later.

For some years simplified solitary wave models have been used for estimates of the characteristics of periodic breaking waves. In this paper several characteristics of breaking solitary and cnoidal waves will be discussed and contrasted to assist in evaluating the adequacy of such models. In that regard, of interest were the change in wave height and wave shape with distance and the growth and decay with distance of the roller generated at breaking for these two types of waves. The latter was given attention because of the relation between the roller characteristics and the vorticity generated in the post breaking region by the wave at breaking. For both solitary and cnoidal waves some comparisons will be made between the characteristics of spilling and plunging breakers. Experiments were conducted in the laboratory using breaking solitary and cnoidal waves with the data collected from detailed visual observations. Thus, a comparison of these waves will be made in a macroscopic context only. The experimental equipment and techniques used will be presented first followed by the presentation and the discussion of the results.

EXPERIMENTAL EQUIPMENT

A tilting wave tank was used for all experiments; the tank is 39.6 m long, 1.1 m wide, and 0.61 m deep and is constructed with glass sidewalls throughout and a stainless steel bottom which is plane to within about ± 1.0 mm. The tank is supported at a central hinge point with two motorized jacks upstream and two downstream, geared to operate together thereby permitting a continuous adjustment of slope from horizontal to a maximum slope of about 1:50. The supports for a bulkhead wave generator located at one end of the tank are an integral part of the wave tank structure and tilts with the tank; in this manner waves can be produced on a slope and caused to break at predetermined locations.

The generator is driven by an electro-hydraulic servo-system with the voltage time history determined so the velocity of the wave plate, at a given time, matches the water particle velocity of the wave as it propagates away from the plate. This wave generation technique has been described by Goring and Raichlen (1980). An iterative procedure can be used to compensate for the dynamics of the mechanical hydraulic system; see Skjelbreia (1987). The general characteristics of solitary waves generated in this tank when horizontal have been described by Lee, Skjelbreia, and Raichlen (1982); and a description of the cnoidal waves and their kinematics generated with the tank horizontal has been given by Raichlen and Lee (1984). As mentioned earlier, to produce breaking waves the wave tank was tilted and both solitary and cnoidal waves wave breaking could be induced at pre-determined locations by modifying the characteristics of the wave plate trajectory, i.e., the relative wave height at the point of generation: (H_0/h_0) , where H is the wave height, h is the depth, and the subscript $_0$ indicates the location is at the wave generator.

It was found by Skjelbreia (1987) that just prior to and at wave breaking, wire resistance wave gages normally used to define the free surface were inaccurate when the free surface changed rapidly with time. Problems using this type of gage increased after breaking when air is entrained. It was apparent that observations made using high speed motion picture techniques would eliminate such questions regarding the gage response and the effect of the variation of the electrical conductance of the air-water mixture. Therefore, the wave shape and wave heights were obtained from the frame-by-frame analysis of projected images of the wave obtained from high speed motion pictures. The 16 mm. camera which was used can operate at film speeds which can be continuously adjusted up

to a maximum of 500 frames per second with adjustable shutter speeds to 1/4000 sec. Timing marks every 1/100 sec. are automatically imaged on the film frames. The camera and the necessary lights were mounted to a carriage which could be moved along precision rails mounted to the walls of the tank. The carriage was moved manually so that the breaking region of the wave was approximately centered in each film frame. This was relatively easy even though the wave speed decreased as the wave approached the shoreline. There was probably an error of about ± 1 mm using this technique due to the meniscus which formed on the sidewall of the tank.

An estimate of the size of the roller on the front face of the breaker was made also using the individual frames of the high speed motion pictures. The cross sectional area of the *bubble mass* was used as a measure of the roller size, and its cross section area was estimated from the projection of the *bubble mass* on the sidewall of the tank as seen in the individual film frames. Only the *bubble mass* seen on the front face of the wave was used for this definition; bubbles appearing further back in the wave were not included in this defined area. Several aspects of this measurement will be discussed more fully later.

RESULTS AND DISCUSSION OF RESULTS

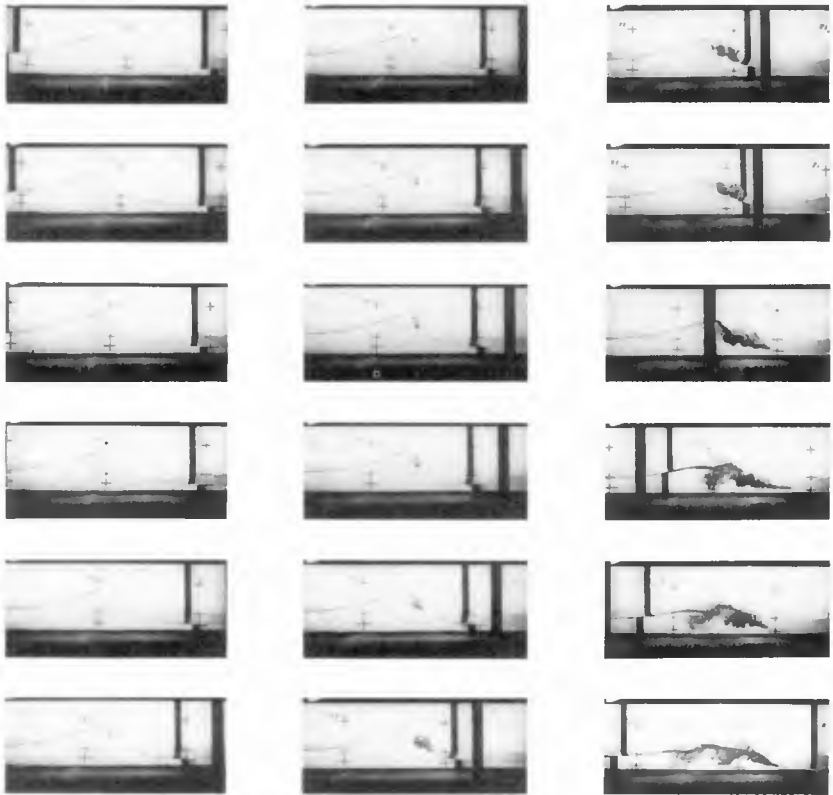
It is instructive, before discussing the more quantitative aspects of wave breaking obtained from the experiments conducted, to view certain features of breaking in a qualitative sense. This can be done from sequences of frames of selected high speed motion pictures taken in the course of the experiments.

A series of frames taken from a 300 frame per second high speed movie of a breaking solitary wave are presented in Figure 1. The solitary wave was generated in the wave tank which was sloped at 0.0191 m/m with a water depth at the wave generator of 43.25 cm; the experiment is denoted as Experiment P-1. In each frame the bottom of the tank can be seen along with the vertical members which support the glass sidewalls. The numbers in each frame indicate distance in meters measured from one end of the tank, and the horizontal bars superposed on the short vertical ones define the still water level for the experiments. (The lowest line corresponds to the still water level for this group of experiments.) The distance between crosses is 50 cm.; for convenience a bar-scale is shown at the bottom of the figure. For reference, the mean position of the wave machine is at Station 37.71 m.

In Figure 1 the sequence of breaking for a plunging breaker can be followed from the position just at breaking (shown in the upper lefthand frame at tank station 22.12 m.) to the post breaking position (shown in the lower righthand frame). Breaking is defined as occurring when the face of the wave in the crest region becomes vertical shortly before overturning takes place. This definition was used for both plunging and spilling breakers. The depth at breaking is: $h_b = 13.50$ cm. and the wave height at breaking is: $H_b = 16.50$ cm as obtained directly from the frame. As one views the sequence of frames, the overturning of the crest and the subsequent formation of the jet just after breaking can be seen as the wave crest approaches $x = 22$ m. The wave propagates shoreward about one breaking depth before the jet impinges with splashup on the front face of the wave. (See the third frame in the center row of photographs.) At that point the wave begins to collapse and change shape while generating the roller on the front face of the wave. The process of the "folding" of the air into the wave can be seen easily. As the wave propagates shoreward it appears to travel through the *bubble mass* as can be seen in the last few photographs of the sequence. The vortical motion so generated can be seen easily. It should be noted that the total distance the wave has travelled in the complete sequence of photographs shown is only about 1.5 m. or about 12 breaking depths.

A qualitative comparison between a breaking solitary wave and a breaking cnoidal wave can be made by reviewing the series of photographs presented in Figure 2. The left-hand column of frames is for the plunging breaking solitary wave which was shown in Figure 1 (Experiment P-1) with the relative distance shoreward of breaking indicated beneath each frame. The right-hand column corresponds to a plunging breaking cnoidal wave (Experiment ACN-4) with the relative shoreward distance from breaking also shown

SOLITARY (EXPERIMENT: P1)



$S = 0.0191 \text{ m/m}$



$h_b = 13.50 \text{ cm}$

$H_b = 16.50 \text{ cm}$

$x_b = 22.12 \text{ m}$

Figure 1 Photographs of a Breaking Solitary Wave, Experiment P1, $S = 0.0191 \text{ m/m}$.

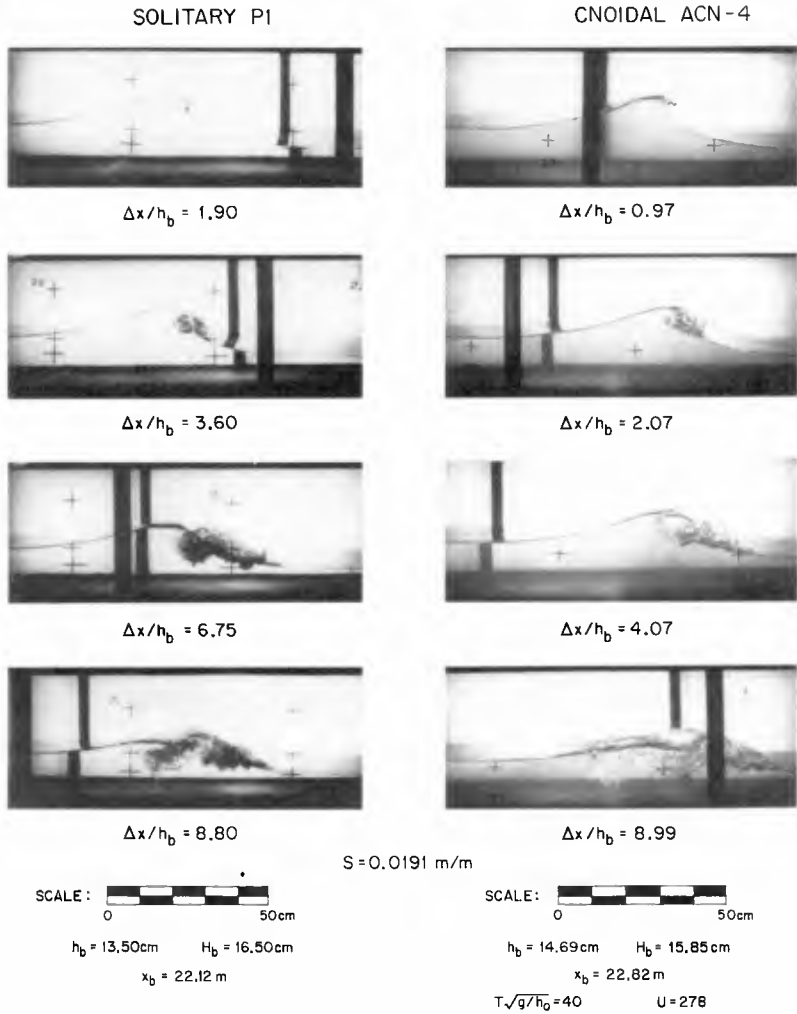


Figure 2 Photographs of a Breaking Solitary Wave (Exp. P1) and a Breaking Cnoidal Wave (Exp. ACN-4).

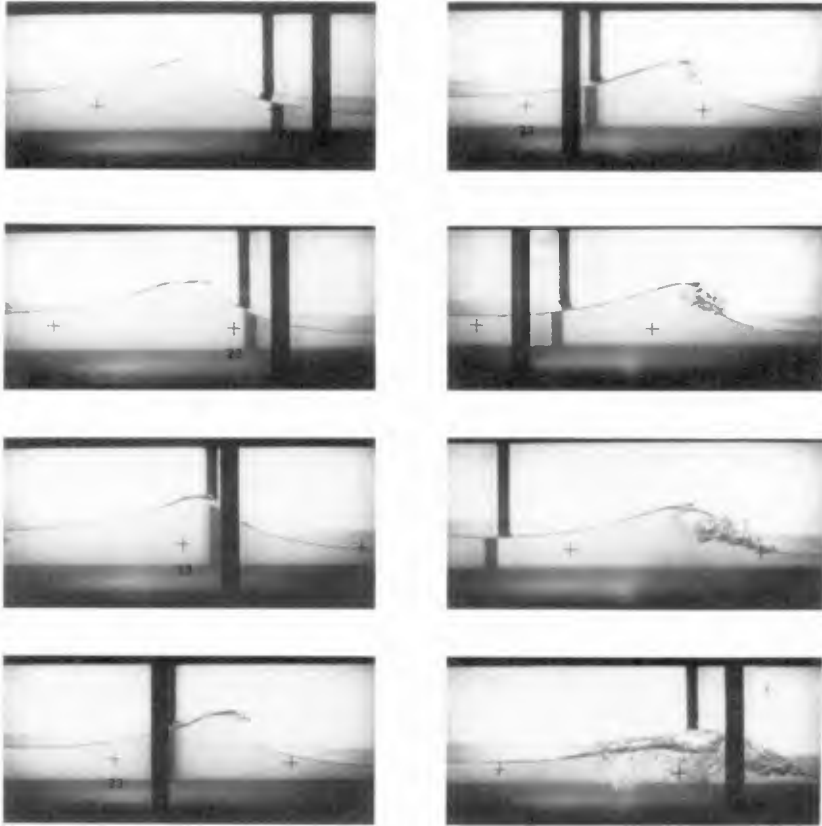
below each frame. In all cases where the results for the cnoidal waves are shown, the photographs and data are for the fourth wave in the wave train. This wave was used as it is far enough back in the wave train so that it appears fully developed and yet not so far back that it would be affected by the reflections from the wave generator of waves which are reflected from the slope. In both cases the flume slope was 0.0191 m/m which is the steepest the wave tank can be tilted. Again the crosses are spaced 50 cm. apart and are located at the still water level; a bar-scale is shown for each sequence of photographs. The cnoidal wave has an Ursell Number at the point of generation which is about 278. (The Ursell Number at the wave generator is defined as: $(HL^2/h^3)_0$, where H is the wave height, h is the water depth, L is the computed wave length.) With that in mind, it is seen, perhaps as would be expected, there are striking similarities between these two types of breaking waves. The solitary wave shows the classic profile of a plunging wave whereas the cnoidal wave shown just to the right, for the locations chosen, shows the jet as it is being ejected from the crest. The shape of the jet appears to be more complex than that for the solitary wave. Certain of the differences observed between the solitary and the cnoidal waves are probably due, for the cnoidal case, to the influence of the prior breaking waves. As waves break they leave behind a turbulent field which, along with the effect of the offshore current generated by the runup and rundown of the waves at the shoreline, must influence the breaking of subsequent waves in the train. Nevertheless, after breaking occurs, the shape of the waves as they propagate shoreward are similar for the two cases. This suggests that the post breaking region is strongly controlled by the details of the flow at the crest during the overturning process. This is probably reasonably similar for the cases shown indicating that the details of the initial wave, i.e., solitary or cnoidal, probably are not too important in this regard.

In Figures 3 and 4, photographs are presented showing the breaking of cnoidal waves with Ursell Numbers, at generation, of 278 and 98.3, respectively, with the wave tank sloped at 0.0191 m/m. In a general way the photographs are similar for both the breaking and post breaking regions. The irregularities near the crest in the second photograph on the left in Figure 3 may be an indication of a wave propagating offshore generated at the shoreline by the runup-rundown process. Further into the sequence it is seen that the broken wave travels through the vortices generated during the breaking process, e.g., see the last photographs of the two sequences. The depth to which the bubbles generated at the water surface during the breaking process penetrate when the wave is greater than ten breaking depths shoreward of the breaking location is somewhat surprising in these figures, as well as in Figure 1 for the solitary wave. (Similar effects have been observed by Nadaoka (1986).) A series of photographs is presented in Figure 4 for the cnoidal wave with an Ursell Number of 98.3 when breaking in the tank with a bottom slope of 0.0191 m/m. There is little difference in the overall features seen in the photographs for similar distances shoreward of breaking for the waves shown in Figures 3 and 4 suggesting that the processes among the three waves: the solitary wave and the two cnoidal waves for the same bottom slope are similar.

The variation of the relative wave height at breaking, $(H/h)_b$, with the bottom slope, S , for the solitary waves and the cnoidal waves which were tested is presented in Figure 5. Plotted next to each data point is the relative wave height at generation: H_0/h_0 . In this figure the nondimensional parameter: $T(g/h_0)^{1/2}$ is used to define the two different cnoidal waves which were used; Table 1 shows the experimental conditions for these cnoidal waves. The slopes were chosen to generate a range of breaking waves from spilling to plunging. The spilling wave occurs at a slope of 0.0061 m/m with a gradual change to plunging at a slope of 0.0191 m/m. This figure demonstrates that the differences between spilling and plunging breakers are not distinct; perhaps they are more related to the *intensity* of the overturning jet associated with breaking rather than major differences in the waves themselves. The interested reader is directed to Papanicolaou and Raichlen (1987) for a discussion of certain of these aspects for the solitary wave.

In Figure 5 self-similarity at breaking for the solitary wave is demonstrated by the three data points shown for a tank slope of 0.0126 m/m. For that case the relative breaking height is essentially the same, independent of the generation conditions. The

CNOIDAL ACN-4



$S = 0.0191 \text{ m/m}$

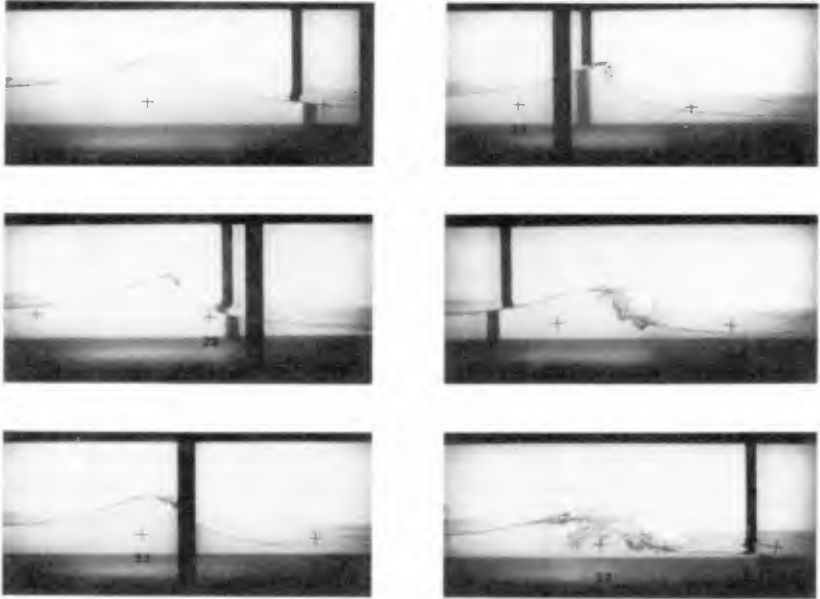
SCALE:  0 50cm

$h_b = 14.69 \text{ cm}$ $H_b = 15.85 \text{ cm}$ $x_b = 22.82 \text{ m}$

At Generation: $T\sqrt{g/h_0} = 40$ $U = 278$

Figure 3 Photographs of a Breaking Cnoidal Wave (Exp. ACN-4).

CNOIDAL ACN-2


 $S = 0.0191 \text{ m/m}$

SCALE :  0 50 cm

 $h_b = 15.05 \text{ cm}$ $H_b = 14.59 \text{ cm}$ $x_b = 23.03 \text{ m}$

At Generation: $T\sqrt{g/h_0} = 25$ $U = 98.3$

Figure 4 Photographs of a Breaking Cnoidal Wave (Exp. ACN-2).

water depth at the location of the wave generator was the same for the three different experiments, hence, the waves break at different locations. An experimental curve is shown for the solitary wave which, if extrapolated, tends to a value of relative height at breaking of about 0.8 for a horizontal bed. The data for the cnoidal waves vary in a similar manner with slope as the corresponding data for the solitary waves. Thus, there appears to be a strong similarity in the trends of relative breaking height with increasing slope for solitary and cnoidal breaking waves. The differences observed between the relative breaking heights of solitary and cnoidal waves for the same slopes are probably related to the influence of the prior breaking waves on the observed wave in the train, i.e., the fourth wave.

Table 1 Experimental Conditions for Cnoidal Waves

Experiment No.	S (m/m)	T(g/h ₀)	(HL ² /h ³) ₀
ACN4	0.0191	40	278.
ACN2	0.0191	25	98.3
ACN7-1,2	0.0061	40	706.
ACN6-1	0.0061	25	263.

In Figure 6 the variation of the breaking wave heights for the cnoidal waves is shown (normalized by the breaking solitary wave height) as a function of the generation Ursell Number for each of two different wave tank slopes. It is interesting to see that the effect of slope does not appear significant for these data even though at the smaller slope the breaking wave is essentially a spilling wave and at the larger slope it is a plunging wave (see Figures 3 and 4).

The variation of the relative wave height, H/H_b , with distance shoreward of breaking, $\Delta x = (x-x_b)$, is presented in a nondimensional manner in Figures 7 and 8 for waves breaking on a slope of 0.0191 m/m and 0.0061 m/m, respectively. (The location of the point of observation is denoted as x and the location of the breaking position is x_b .) For each tank slope, data are shown for solitary and cnoidal waves with different non-dimensional generation times. It should be mentioned, after breaking the wave height defined corresponds to the height for the portion of the wave which appears to have little air entrained. If, for example, one refers to the last frame presented in Figure 4, it is seen that the height of the roller (or *bubble mass*) is somewhat greater than that corresponding to the clearer region behind; the height used in Figure 7 corresponds to the latter. As seen in Figures 7 and 8, and also best shown in the photographs presented in Figure 2, both the cnoidal and the solitary waves propagate some distance shoreward of breaking with little effect on the wave height. This is in accord with the observations of Galvin (1968), (1969); the Shore Protection Manual of the U.S. Army Corps of Engineers (1984) follows these observations and recommends that the post-breaking distance during which the wave height changes only slightly be defined as: $(\Delta x/h_b) = (4 - 9.25S)(H/h)_b$. For the solitary wave of Figure 7 the distance computed from this expression is about 4.7.

Figure 7 shows that, for the solitary wave, at a location of about five breaking depths the rate of change of the wave height with distance begins to increase. For the two cnoidal waves, i.e., $U = 98.3$ and 278, there is a more rapid decrease in relative wave height with distance shoreward of $\Delta x/h_b = 3$ than for the solitary wave. This is probably due to the influence of the preceding waves on the breaking process. This can be seen easily in Table 2 where the exponent, n , in the expression: $(H/H_b) \sim (\Delta x/h_b)^n$ is presented for the various experiments for $4 < \Delta x/h_b < 8$. Thus, these data indicate an increase in the energy dissipation in the post breaking region of periodic waves compared to solitary waves. The data shown in Figure 7 for the region of $7 < \Delta x/h_b < 15$ shows a relatively constant relative wave height of about $H/H_b = 0.5$. This is the beginning of the region where a bore is formed and the wave height changes more slowly. Horikawa and Kuo (1966) show, in this bore region, that the wave height relative to the local water depth

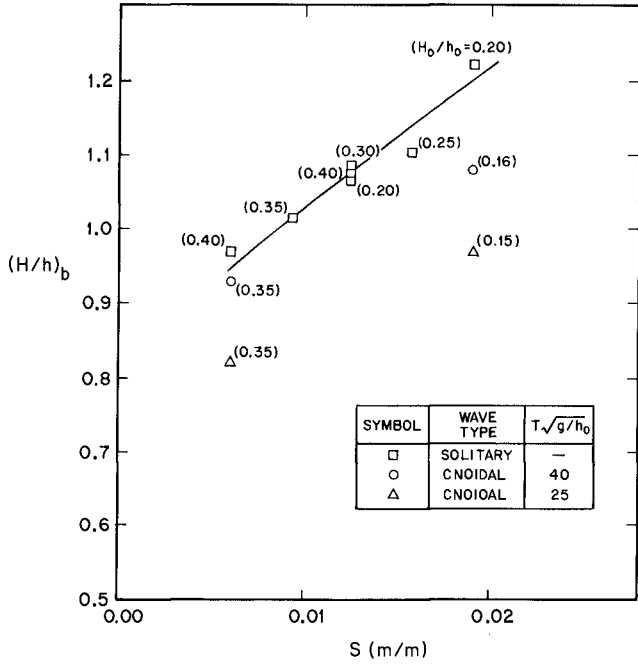


Figure 5 Variation of Relative Height at Breaking with Bottom Slope.

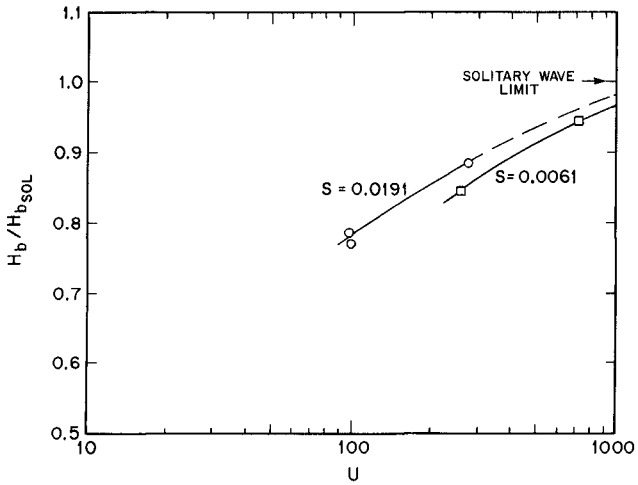


Figure 6 Variation of Relative Height and Breaking with Ursell Number at Generation.

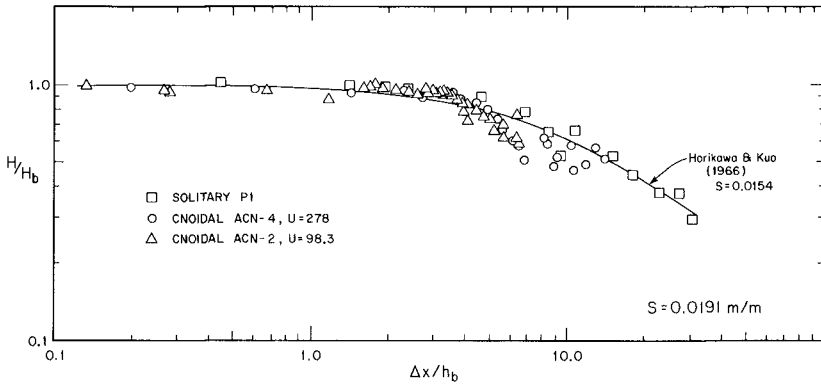


Figure 7 Variation of Relative Height after Breaking with Relative Distance ($S = 0.0191$ m/m).

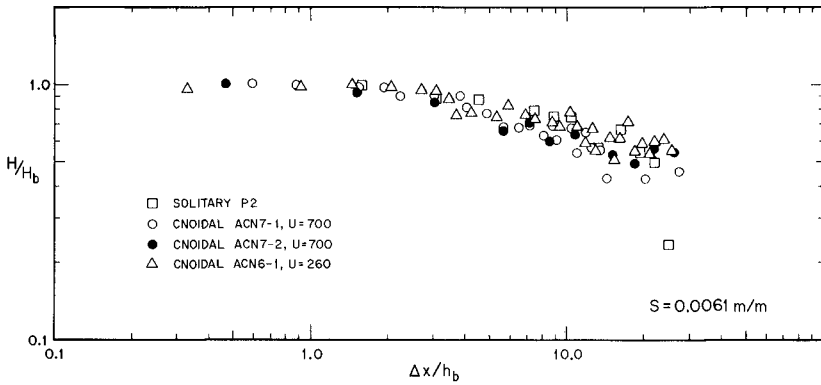


Figure 8 Variation of Relative Height after Breaking with Relative Distance ($S = 0.0061$ m/m).

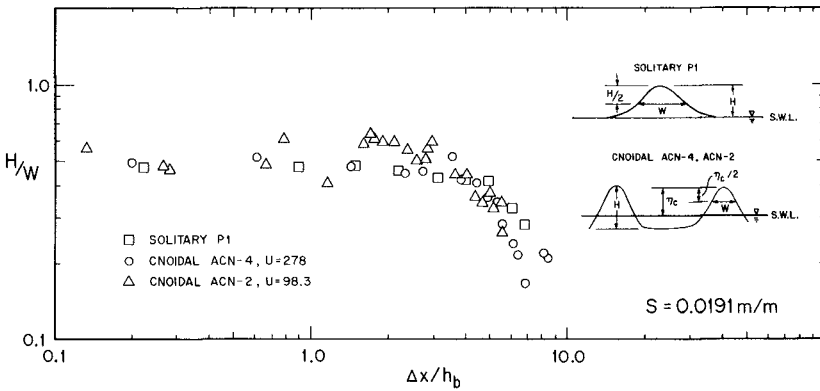


Figure 9 Variation of Aspect Ratio of Wave after Breaking with Relative Distance ($S = 0.0191$ m/m).

asymptotically approaches a constant value of between 0.35 and 0.4 for certain of their experiments. A curve is presented which corresponds to the experimental data from

Table 2 The Exponent n for the Various Experiments

Experiment Number	n
P1	- 0.621
ACN4	- 1.01
ACN2	- 0.769
SP2	- 0.521
ACN7-1,2	- 0.398
ACN6	- 0.382

Horikawa and Kuo (1966) for periodic waves breaking on a slope of 0.0154 for the region of data from these experiments. (Similar data have been presented by Svendsen et al (1978) for periodic waves breaking on a slope of 0.0292.)

In Figure 8 the variation of relative wave height with distance is presented for a solitary wave and for two cnoidal waves with Ursell Numbers of about 700 and 260 breaking on a bottom slope of 0.0061 m/m. Instead of the plunging waves in Figure 7, the waves break as spilling breakers. The first observation is that for $\Delta x/h_b \geq 3$ the rate of decrease in the relative wave height is less for the spilling breaker than it is for the plunging breaker. This has been shown, with reference to the exponent, n , in Table 2. In fact, for the spilling breaker the relative change in wave height with distance shoreward of breaking is *similar* for the solitary and two cnoidal waves shown; actually the rates are somewhat less for the cnoidal waves as compared to the solitary wave. For the spilling waves the relative wave height becomes approximately constant at about $H/H_b = 0.5$ to 0.6 for: $15 \leq \Delta x/h_b \leq 25$ which, similar to the plunging wave case, is where the broken waves become bores and propagate shoreward with a smaller change in relative height. The consistency of the data acquisition and analysis is shown by the agreement of the data for Experiments ACN 7-1 and ACN 7-2 conducted at separate times with the same experimental conditions. It is interesting to observe that the rate of change of relative wave height with distance for the spilling and plunging solitary waves shown in Figures 7 and 8 are similar.

It was realized from reviewing the motion pictures that the change in wave height in the initial region after breaking was related also to the change in the wave shape in addition to the effects of energy dissipation. However, the effects of energy dissipation must not be too great in the region just after breaking, since in that region the overturning crest associated with the breaking process has not had time to fully generate the vortical motion observed further shoreward of breaking. To explore this with the data available from the current experiments, an aspect ratio of the wave was used which was defined as the ratio of the wave height, H , to the width of the wave, W , measured one half of the distance from the still water level to the crest. The variation of H/W with relative distance from breaking, $\Delta x/h_b$, is presented in Figure 9 for plunging breaking solitary and cnoidal waves. (A definition sketch for the width, W , is shown in the inset.) For this slope, i.e., $S = 0.0191$ m/m, the Ursell Numbers for the two cnoidal waves are 98.3 and 278, respectively. In the region from breaking to about two breaking depths shoreward of breaking the aspect ratio is relatively constant and equal to between about 0.5 and 0.6 for both the solitary and the cnoidal waves. There is a relatively gradual decrease in H/W for the solitary wave when $2 \leq \Delta x/h_b \leq 5$; for $\Delta x/h_b > 5$ the aspect ratio decreases more rapidly. In the case of the two cnoidal waves similar changes take place. If the variation of the aspect ratio with distance for this rapidly changing region is expressed as: $(H/W) \sim (\Delta x/h_b)^n$; the exponent n for experiments: P1, ACN4, and ACN2 are - 1.285, - 1.43, and - 1.17, respectively. Within the errors involved in the definition of the aspect ratio, it appears that the decrease in the aspect ratio with distance in this rapidly changing region is

similar for each of the three different waves.

Svendsen (1984) and Duncan (1981) have given attention to the size of the roller generated during the breaking process. Measurements were reported by Duncan (1981) using a breaker which was generated by a towed hydrofoil. These results were used by Svendsen (1984) to estimate the percentage of energy dissipated from breaking through the region referred to by him as the transition region. However, the experiments reported by Duncan (1981) were essentially steady ones, i.e., the hydrofoil moved at a constant velocity, whereas the wave breaking process is highly unsteady.

As mentioned in the previous section, the variation in roller size was determined in this study as a function of distance from breaking using the high speed motion pictures taken with the camera following the wave. The roller area was defined using the projection on the side of the wave tank of the area of the *bubble mass* which travels on the front face of the breaker. Obviously this technique can only provide an estimate of the roller area, but if it is done consistently, a comparison of this area can be made among the different types of waves used in these experiments. Examples of these projected areas can be seen easily in the photographs presented in Figures 1 through 4. There is some lateral variation to the *bubble mass*, as can be seen in the frame corresponding to $\Delta x/h_b = 8.99$ in Figure 2, so the technique used yields simply an *estimate* of the roller size. This is a crude measurement of the roller area, but at the very least it provides one other way by which the breaking process of solitary and cnoidal waves can be compared.

In Figure 10 the variation of the cross section area of the *bubble mass* normalized by the square of the breaking wave height, A/H_b^2 , is presented as a function of the relative distance shoreward of breaking, $\Delta x/h_b$, for a plunging solitary wave and two cnoidal waves breaking in the wave tank sloped to 0.0191 m/m. It is seen that, for the cases shown, the maximum value of the relative area is close to unity. The average value of the normalized roller area reported by Duncan (1981) from his steady experiments was: $A/H_b^2 = 0.86$. The *bubble mass* area ratio reaches a maximum between about seven and ten breaking depths shoreward of breaking. (The interested reader is directed to Papanicolaou and Raichlen (1987) for more detailed information on *bubble mass* areas for solitary waves.) Referring back to Figure 7, for the cnoidal waves, the maximum appears to be reached *after* the wave height has decreased at its maximum rate to the observed *plateau* in height. As would be expected, the area of the bubble mass increases significantly over the distance that the height is changing the most, i.e., for: $3 < \Delta x/h_b < 8$ the relative roller area increases by a factor of ten. The data for the solitary waves and the cnoidal waves with Ursell Numbers of 98.3 and 278 are quite similar in trend and in the maximum relative bubble areas.

The growth of the roller, i.e., the *bubble mass*, for spilling breakers was investigated also, and the results are presented in Figure 11. With the wave tank sloped to 0.0061 m/m both the solitary wave and the two cnoidal waves broke as spilling breakers where the overturning at the crest was observable but certainly not as dramatic as for the waves breaking on the steeper slope. The data from two different experiments for the same conditions, i.e., $U = 700$, are in good agreement indicating that comparisons of *bubble mass* areas made among the different waves are reasonable. In comparing the relative roller area for the solitary wave to that observed for the cnoidal waves it was found that there was very little difference in the trend of the data. The relative areas grew from about 0.1 to a maximum for: $2 < \Delta x/h_b < 10$. However, unlike the plunging breakers, the maximum relative areas are somewhat different. They range from about 0.5 to 0.6 for the cnoidal waves to 0.8 for the solitary waves. Although this may be within the range of the accuracy of the data reduction, it is also possible (and reasonable) that the rate of growth of the roller is slower for the spilling breaker compared to the plunging breaker. Thus, assuming this area is related to the associated energy dissipation, Figures 10 and 11 support the generally held hypothesis that the energy dissipation for spilling breakers is less than that for plunging breakers. This also agrees with the observations made in comparing Figures 7 and 8 for the change in relative wave height after breaking.

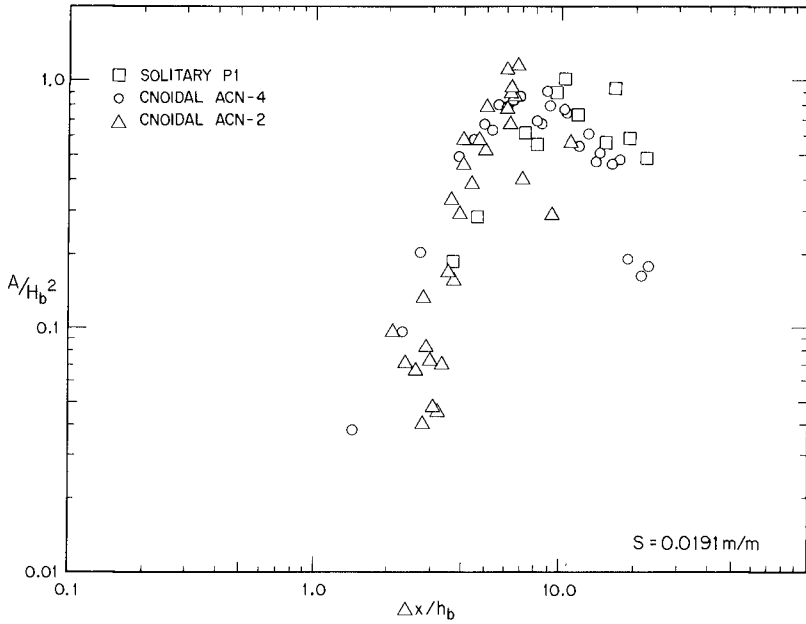


Figure 10 Variation of Relative Bubble Mass after Breaking with Relative Distance ($S = 0.0191 \text{ m/m}$).

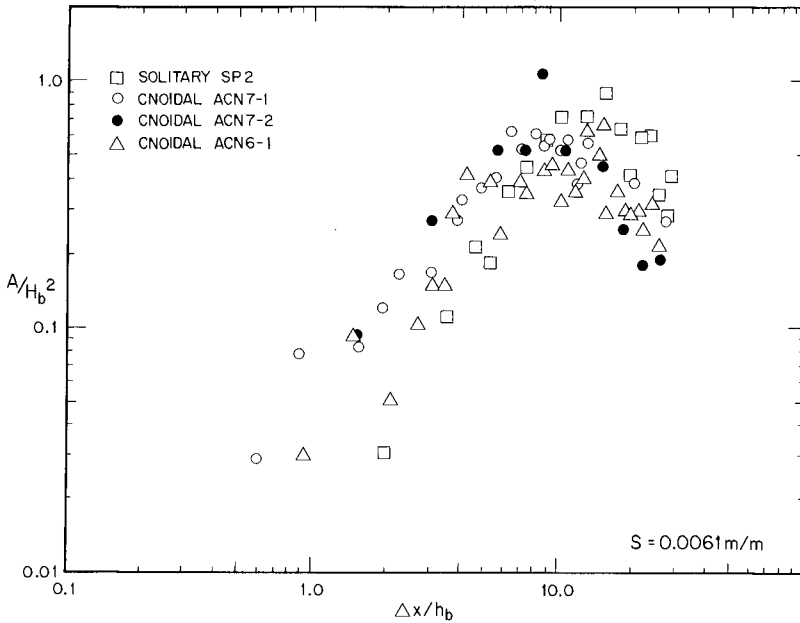


Figure 11 Variation of Relative Bubble Mass after Breaking with Relative Distance ($S = 0.0061 \text{ m/m}$).

Conclusions

The following major conclusions may be drawn from this study:

1. The data for breaking solitary and cnoidal waves each show plunging waves differ from spilling waves primarily in the *rate* of change of the properties investigated, not in overall characteristics.
2. The relative breaking height $(H/h)_b$, for the solitary and cnoidal waves tested, increases with slope and for a given slope the relative breaking wave height is a maximum for solitary waves compared to the cnoidal waves.
3. The breaking of a solitary wave which is between a spilling and a plunging breaker is self-similar.
4. There is a region of three to five depths shoreward from breaking where the wave height is relatively unchanged, followed by a region of three to five breaking depths over which major changes in wave height and shape take place. It was apparent from the data that the changes in height for the cnoidal waves with distance after breaking was significantly greater for the plunging waves compared to the spilling waves. The comparable changes for the solitary waves (plunging and spilling) were similar.
5. The aspect ratio of the wave, H/W , changes in a manner similar to the height. For the plunging case, for which this was defined, the decrease of the aspect ratio in the rapidly changing region was similar for the solitary and the two cnoidal waves.
6. The *bubble mass* on the front face of the wave grows from zero, reaches a maximum, and decreases; the maximum relative size of the mass expressed as A/H_b^2 is of the order of unity.
7. Solitary and cnoidal waves exhibit reasonably similar changes in wave height and *bubble mass* for each type of breaking wave investigated (spilling or plunging) indicating that effects on the waves of breaking for these translatory and oscillatory waves may be similar.

Acknowledgement

The writers appreciate the support of the National Science Foundation through Grant : MSM-8311374 and by the Miriam and Omar J. Lillevang Fund at Caltech.

References

- Battjes, J.A., "Surf-Zone Dynamics", Ann. Rev. Fluid Mech., 20:257-93, 1988
- Dally W.B., Dean, R.G., and Dalrymple, R.A., "Modeling Wave Transformation in the Surf Zone", Misc. Paper CERC-84-8, Coastal Engineering Research Center, Waterways Exp. Sta., 1984
- Duncan, J.H., "An Experimental Investigation of Breaking Waves Produced by a Towed Hydrofoil", Proc.R.Soc.Lond., A377, 331-348, 1981
- Galvin, C.J., Jr., "Breaker Type Classification on Three Laboratory Beaches", Journ. of Geophysical Res., Vol. 73, No. 12, 1968
- Galvin, C.J., Jr., "Breaker Travel and Choice of Design Wave", Journ. of Waterways and Harbors Div., ASCE, WW2, 1969
- Goring, D.G. and Raichlen, F., "The Generation of Long Waves in the Laboratory", Proc. of the Seventeenth Coastal Engineering Conf., Sidney, Australia, 1980

- Horikawa, K. and Kuo, C-T, "A Study on Wave Transformation Inside the Surf Zone", Proc of the Tenth Conf. on Coastal Engr., Tokyo, Japan, 1966
- Lee, J.-J., Skjelbreia, J.E., and Raichlen, F., "Measurement of Velocities in Solitary Waves", Journ.of Waterways, Ports, Coastal and Ocean Div., ASCE, Vol. 108, No. WW2, pp.200-218, May 1982
- Nadaoka, K., "A Fundamental Study on Shoaling and Velocity Field Structure of Water Waves in the Nearshore Zone", Tech. Rpt. No. 36, Dept. of Civil Engr. Tokyo Institute of Technology, 1986
- Papanicolaou, P. and Raichlen, F., "Wave Characteristics in the Surf Zone", Coastal Hydrodynamics, ASCE, University of Delaware, 1987
- Peregrine, D.H., "Breaking Waves on Beaches", Ann. Rev.Fluid Mech., 15:149-78, 1983
- Peregrine, D.H. and Svendsen, I.A., "Spilling Breakers, Bores, and Hydraulic Jumps", Proc. of the Sixteenth Coastal Engr. Conf., Hamburg, Germany, 1978
- Raichlen, F. and Lee, J.-J., "The Interaction of Small and Finite Amplitude Long Waves and Currents", Proc. of the Nineteenth Conf. on Coastal Engr., Houston, Texas, 1984
- Shore Protection Manual, Coastal Engr. Res. Center, U.S.Army Corps of Engrs., 1984
- Skjelbreia, J.E., "Observations of Breaking Waves on Sloping Bottoms by Use of Laser Doppler Velocimetry", Report No. KH-R-48, W.M.Keck Laboratory of Hydraulics and Water Resources, Calif. Inst. of Tech., 1987
- Svendsen, I.A., "Wave Heights and Set-Up in a Surf Zone", Coastal Engineering, Vol. 8, 1984
- Svensen, I.A., Madsen, P.Å., and Hansen, J.B., "Wave Characteristics in the Surf Zone", Proc. of the Sixteenth Coastal Engr. Conf., Hamburg, Germany, 1978